

# APPLICATION OF MEASUREMENT METHODS FOR THE FREQUENCY RANGE 2-150 KHZ TO LONG-TERM MEASUREMENTS IN PUBLIC LOW VOLTAGE NETWORKS

*Victor Khokhlov<sup>1\*</sup>, Jan Meyer<sup>1</sup>, Deborah Ritzmann<sup>2</sup>,  
Stefano Lodetti<sup>2</sup>, Paul S Wright<sup>2</sup>, David de la Vega<sup>3</sup>*

<sup>1</sup> *Institute of Electrical Power Systems and High Voltage Engineering  
Technische Universität Dresden, Dresden, Germany*

<sup>2</sup> *National Physical Laboratory, Teddington, UK*

<sup>3</sup> *Department of Communications Engineering,  
University of the Basque Country (UPV/EHU), Bilbao, Spain,*

*\*victor.khokhlov@tu-dresden.de*

**Keywords:** DISTORTION MEASUREMENT, ELECTROMAGNETIC COMPATIBILITY, MEASUREMENT STANDARDS, POWER QUALITY, SUPRAHARMONICS

## Abstract

This paper studies the feasibility of selected measurement methods in the frequency range 2-150 kHz in the application to long-term field measurements. Disturbance measurements over days and weeks carried out at different sites in public low voltage networks provide the basis for analysis. Measurements are taken continuously and cover the typical variation of disturbance levels caused by the changing operating points of the connected disturbance sources. The analysis focuses on the suitability of obtained measurement results for different objectives, namely reflection of relevant interference mechanisms and assessment against compatibility levels. The paper summarizes the results of the analysis and intends to provide input for the present activities in IEC SC77A WG9 to define a normative measurement method for network measurements in the frequency range 2-150 kHz to be included in the next edition of IEC 61000-4-30.

## 1. Introduction

Advances in power electronics, increasing share of renewables and e-mobility lead to a shift of emission from lower to higher frequencies. While the low order harmonic distortion is usually reduced, end-users and network operators face an increase in emission in the frequency range 2-150 kHz, which is referred to as supraharmic emission. Despite the relevance of this problem and the attention that it is drawing in the research community, the coordination of electromagnetic compatibility (EMC) in this frequency range is incomplete. Its essential part is a credible and agreed framework for measuring the emission of electrical equipment and disturbance levels seen in the network. At the present state of standardisation, a normative method to measure the emission of equipment under laboratory conditions, also known as CISPR method, is defined in [1]. Recently published compatibility levels in the frequency range 9-150 kHz [2], which are focused mainly on protecting Power Line Communication (PLC) systems, refer to the CISPR method as well. The normative method for measurement of disturbance levels in the network is lacking and its definition is in the scope of present activities of IEC SC77A WG9.

Several measurement methods are currently under discussion [3]. These methods have individual benefits and drawbacks, and a recommendation for one specific method is hardly possible. The decision depends on the objectives of disturbance measurements in the network, which may include the assessment of disturbance levels against compatibility levels and reflection of relevant interference mechanisms (i.e. additional thermal impact or malfunction). While the first is associated with applying the CISPR method, the method specified in the standard IEC 61000-4-7 [4] effectively represents the second aspect.

The suitability of the methods for both use cases has not been addressed yet. This paper evaluates the methods focusing on their ability to reflect relevant interference mechanisms and enable the comparison with compatibility levels simultaneously. The analysis is based on measurements over days and weeks in environments with typical disturbance sources and considers different aspects of applying the methods to the long-term measurement in the network.

The paper starts with a description of the measurement methods and associated methodology. Next, the analysis framework introduces the measurement procedure and provides an overview of the measurements sites. The results are discussed for the different disturbance sources separately before the conclusion of the study is provided.

## 2. Measurement Methods

### 2.1. CISPR 16-1-1

The standard specifies instrument characteristics of a measurement receiver for emission measurement at frequencies above 9 kHz, including the CISPR Band A (9-150 kHz). Application of the measurement receiver is normative for measurement of electronic equipment emission in the laboratory.

The measurement receiver employs the principle of a heterodyne spectrum analyser, whose output is processed with a quasi-peak (QP) detector. The QP detector represents an RC-circuit followed by a critically damped meter and weights the signal envelope upon its duration and repetition rate. This feature underlines the original idea behind the design of the measurement receiver, namely the ability to reflect the impact of peaks in the emission on radio transmission systems.

The measurement result is the maximum QP value ( $QP_{max}$ ) of emission observed by the receiver over the whole measurement duration. It implies a two-stage emission assessment process, including orientation measurements and detailed measurements to obtain the worst-case operation point of equipment under test. Additionally, it requires the usage of Line Impedance Stabilization Network (LISN) to prevent the incoming disturbances from the mains supply and ensure the specified impedance at the terminal of the equipment under test.

The specification of instrument characteristics allows significant flexibility in the compliant implementation of the measurement receiver. Since 2010, the standard allows digital DFT-based implementations along with classical analogue receivers. Although this enables parallel measurement at multiple frequencies simultaneously, it also sets high performance requirements. Initial comparison, conducted by the authors of this paper, showed that both computational complexity and memory costs are expected to be at least one magnitude order higher than for the measurement method specified in IEC 61000-4-7.

In addition, tolerance bands for analogue receivers also apply to digital implementations. Accordingly, compliance tests provided in the standard permit uncertainty requirement of up to  $\pm 2$  dB, which results in a -21/+26 % possible deviation range.

### 2.2. IEC 61000-4-7

A method for measuring emission in the frequency range 2-9 kHz is specified in the informative Annex B of the standard. It is intended for emission measurement of electronic equipment but is also widely applied for the measurement of disturbance levels in the field.

The method specifies a measurement interval of 200 ms (rectangular window) independent of the nominal frequency for processing by a Discrete Fourier Transform (DFT). It results in a discrete spectrum of Root Mean Square (RMS) values with 5 Hz frequency resolution. The spectral components are grouped in 200 Hz bands using the Root Sum Square (RSS) to ensure a comparability with the CISPR Band A definition.

In its normative part, the standard deals with the measurement methods for harmonics and interharmonics, which use proven methodologies for the evaluation of grid disturbance levels. First, basic values calculated over a measurement interval of 10/12 power cycles, i.e. approximately 200 ms, are aggregated in time according to IEC 61000-4-30 [5]. Standard aggregation periods are 150/180 cycles, i.e. approximately 3 s and 10 min. The 3-s value relates to very short occurring emission and consequently to malfunctions, while the 10-min period is linked to the typical thermal time constants of equipment and consequently to additional thermal stress. For comparison to respected disturbance limits, 95 % percentile weekly values for 10-min values and 99 % percentile daily values for 3-s values are commonly used.

## 3. Analysis Framework

### 3.1. Implementation of measurement methods

Informative annex of the standard IEC 61000-4-30 suggests the use of high-pass and low-pass filters for obtaining accurate and reproducible results in the frequency range 9-150 kHz. A high-pass filter reduces spectral leakage by damping the fundamental component and low order harmonics from the input signal, whereas the low-pass filter prevents the anti-aliasing effect by removing components above the frequency range of interest. The high-pass filter can be part of the signal processing stage (digital filters), while the low-pass filter is included in the measurement chain. In this study an analogue low-pass filter (Butterworth characteristic) and a digital Elliptic high-pass filter [6] are applied to the raw measurement data before their further processing.

*3.1.1 CISPR method:* Digital DFT-based implementation of the measurement receiver shall ensure compliance with requirements specified in the standard. It includes frequency selectivity and calibration tests with a sine wave and sequence of pulses with varying repetition frequency. The frequency selectivity of a digital implementation is determined by choice of a window function, which defines the shape of the measurement bandwidth in the frequency domain. A bandwidth  $BW_{-6dB}$  of 200 Hz and a side-lobe attenuation within the limits of CISPR Band A can be achieved by different window functions, such as Gaussian, Lanczos or Kaiser. The implementation used in this study follows the recommendations of IEC and employs Gaussian window function [7]. The parameter  $\alpha$  of the window is set to 5.8.

The digital implementation requires a frequency resolution of 100 Hz or higher and an overlap of more than 75 % in the time domain to pass calibration requirements. The implementation used in this study utilizes measurement intervals of 20 ms with an overlap of 90 %, which results in measurement values with 50 Hz frequency resolution and 2 ms time resolution. For better comparability of results, only measurement values associated with centre frequencies starting at 2.1 kHz in steps of 200 Hz are considered for further analysis. The implementation of the QP detector uses the principles of a digital model [8]. In line with the existing methodology, the measurement result is the  $QP_{max}$  value observed by the digital implementation during the entire measurement period.

3.1.2 IEC 61000-4-7: An extension of the method to the frequencies above 9 kHz is considered in this study to introduce a continuity of standardisation framework for the measurement of network disturbances in the frequency range of interest. Considering the Nyquist criterion, the minimum sampling rate in this case must exceed 300 kHz. If the 200 ms window would be used, the size of a single DFT would increase significantly, affecting both computational and memory requirements. Therefore, shorter measurement intervals are introduced to keep the DFT-size reasonably small, which reduces computational and memory requirements as well as improves the assessment of disturbance characteristics in time.

For better comparability with CISPR method, measurement intervals of 20 ms are used. It results in a discrete spectrum of RMS values with 50 Hz frequency resolution, which are grouped in 200 Hz bands using the RSS. Ten measurement intervals are required to maintain the analysis interval of 200 ms and to cover it gapless. The intermediate ten 20-ms values are aggregated to 200-ms values using both RMS and maximum aggregation.

Further, basic 200-ms values are aggregated in time using a two-stage principle. The 3-s stage exploits 15 basic 200-ms values, while the 10-min stage exploits 200 aggregated 3-s values. Both RMS and maximum aggregation methods are considered to explore their relevance for the objectives of the study. Among twelve possible variants illustrated in Fig. 1, the consecutive aggregation of basic RMS values (*A* and *E*) reflects thermal impact, while the consecutive maximum aggregation of basic maximum values (*D* and *L*) is used as a reference for the perceptible malfunctions [9].

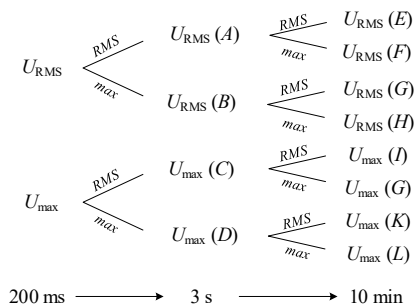


Figure 1 Aggregation variants

### 3.2. Field measurements

The measurement methods described above are implemented on a suitable hardware platform in order to test them over longer durations, because possibility to store raw sample data at high sampling rates and process it offline is limited by space and computation requirements. The prototype instrument is installed at different sites in public low voltage networks in Germany. The voltage measurements are taken continuously with a sampling rate of 1 MHz at the connection points of typical disturbance sources including photovoltaic (PV) inverters and electric vehicle (EV) chargers.

Fig. 2 exemplarily shows the RMS spectra of measured disturbances. For purposes of the study, the spectra and the measurement results are presented as absolute values in V, despite of common representation of disturbance levels above 9 kHz in the logarithmic unit  $\text{dB}_{\mu\text{V}}$ .

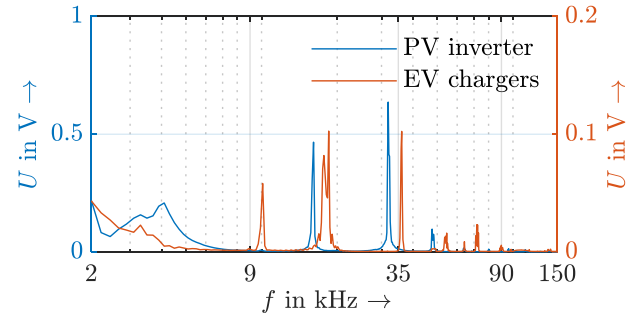


Figure 2 Frequency spectra of disturbances

First measurement is performed at the terminal of a customer installation with a single-phase PV inverter in a rural network during an autumn week. Fig. 2 indicates distinct disturbances at the switching frequency of the inverter around 16 kHz and its second harmonic around 32 kHz. The magnitude of disturbances varies in time and occurs for approximately 11 hours every day. It disappears from dusk until dawn while the inverter is switched off.

Second measurement is performed at the transformer busbar supplying a charging infrastructure with four fast (DC) and one slow (AC) charging points in an urban network during a working day. Fig. 2 indicates distinct disturbances at 10 kHz (switching frequency of an on-board charger), 18 and 36 kHz (switching frequency of a fast charger and its second harmonic). The magnitude of disturbances varies in time and occur only if a car is charging. Five non-simultaneous charging processes with an overall duration of approximately 200 minutes are observed on the day of measurement.

## 4. Measurement Results

### 4.1. Analysis procedure

The results of disturbance measurements of PV inverter and EV chargers are discussed separately. For each measurement the  $\text{QP}_{\text{max}}$  value with CISPR method is determined. Next, the extension of IEC 61000-4-7 method is applied and selected percentile values are calculated for different aggregation variants (cf. Fig. 1).

Main objectives of the analysis are identification of suitably conservative estimator for  $\text{QP}_{\text{max}}$  as basis for the assessment of compliance with compatibility levels as well as demonstration of ability of  $\text{QP}_{\text{max}}$  to represent important interference mechanisms (thermal impact, malfunction). For this reason, the measurement results in Tables 1 and 2 are presented as relative deviation in percentage from the respective  $\text{QP}_{\text{max}}$  values. Colour coding indicates following deviation ranges:  $\pm 5\%$  (green),  $\pm 10\%$  (yellow) and more than  $-10\%$  (red).

Table 1. Relative deviation of results from  $QP_{max}$  in percentage (PV inverter)

| Label | Interval | Basic value | Aggregation |        | 16 kHz |      |       | 32 kHz |      |       |
|-------|----------|-------------|-------------|--------|--------|------|-------|--------|------|-------|
|       |          |             | 3 s         | 10 min | 95 %   | 99 % | 100 % | 95 %   | 99 % | 100 % |
| -     | 200 ms   | $U_{RMS}$   | -           | -      | -3     | -1   | 19    | -3     | 1    | 16    |
| -     |          | $U_{max}$   | -           | -      | 2      | 5    | 29    | -2     | 2    | 26    |
| A     | 3 s      | $U_{RMS}$   | R           | -      | -4     | -2   | 10    | -3     | 1    | 14    |
| B     |          |             | m           | -      | -1     | 1    | 19    | -1     | 3    | 16    |
| C     |          | $U_{max}$   | R           | -      | 2      | 4    | 15    | -2     | 1    | 15    |
| D     |          |             | m           | -      | 6      | 9    | 29    | 0      | 4    | 26    |
| E     | 10 min   | $U_{RMS}$   | R           | R      | -5     | -4   | -3    | -8     | -4   | -1    |
| F     |          |             | m           | m      | 1      | 4    | 10    | 6      | 11   | 14    |
| G     |          |             | R           | R      | -2     | -1   | 0     | -6     | -1   | 1     |
| H     |          |             | m           | m      | 4      | 10   | 19    | 10     | 14   | 16    |
| I     |          | $U_{max}$   | R           | R      | 1      | 2    | 3     | -7     | -3   | 0     |
| J     |          |             | m           | m      | 6      | 10   | 15    | 7      | 11   | 15    |
| K     |          |             | R           | R      | 4      | 5    | 6     | -5     | 0    | 2     |
| L     |          |             | m           | m      | 14     | 19   | 29    | 11     | 16   | 26    |

 Table 2. Relative deviation of results from  $QP_{max}$  in percentage (EV chargers)

| Label | Interval | Basic value | Aggregation |        | 10 kHz |      |       | 18 kHz |      |       | 36 kHz |      |       |
|-------|----------|-------------|-------------|--------|--------|------|-------|--------|------|-------|--------|------|-------|
|       |          |             | 3 s         | 10 min | 95 %   | 99 % | 100 % | 95 %   | 99 % | 100 % | 95 %   | 99 % | 100 % |
| -     | 200 ms   | $U_{RMS}$   | -           | -      | -23    | -9   | 18    | -42    | -27  | 12    | -38    | -22  | 10    |
| -     |          | $U_{max}$   | -           | -      | -22    | -8   | 19    | -42    | -26  | 23    | -37    | -21  | 22    |
| A     | 3 s      | $U_{RMS}$   | R           | -      | -23    | -9   | 18    | -42    | -28  | -6    | -37    | -24  | 9     |
| B     |          |             | m           | -      | -22    | -8   | 18    | -42    | -21  | 12    | -33    | -15  | 10    |
| C     |          | $U_{max}$   | R           | -      | -22    | -8   | 19    | -42    | -27  | -6    | -36    | -24  | 9     |
| D     |          |             | m           | -      | -22    | -7   | 19    | -41    | -20  | 23    | -33    | -12  | 22    |
| E     | 10 min   | $U_{RMS}$   | R           | R      | -23    | -9   | -4    | -49    | -34  | -31   | -41    | -25  | -19   |
| F     |          |             | m           | m      | -18    | 5    | 18    | -31    | -7   | -6    | -25    | 2    | 9     |
| G     |          |             | R           | R      | -23    | -8   | -3    | -44    | -26  | -23   | -39    | -13  | -4    |
| H     |          |             | m           | m      | -18    | 5    | 18    | -31    | 5    | 12    | -24    | 5    | 10    |
| I     |          | $U_{max}$   | R           | R      | -23    | -8   | -3    | -48    | -34  | -30   | -41    | -24  | -18   |
| J     |          |             | m           | m      | -18    | 6    | 19    | -31    | -7   | -6    | -24    | 2    | 9     |
| K     |          |             | R           | R      | -22    | -8   | -2    | -44    | -25  | -23   | -38    | -12  | -3    |
| L     |          |             | m           | m      | -15    | 7    | 19    | -30    | 9    | 23    | -14    | 6    | 22    |

#### 4.2. PV inverter

The results are presented in Table 1. The  $QP_{max}$  values observed at the frequencies with highest disturbance levels during the measurement period of one week are 0.579 V (16 kHz) and 0.786 V (32 kHz). Both values are well below the compatibility levels for non-intentional emission (2.2 V and 1.2 V respectively).

As shown in Table 1, the  $QP_{max}$  tends to exceed the results of consecutive RMS aggregation (A and E). The relative deviation increases with the aggregation time and amounts -8 % for the 95<sup>th</sup> percentile of 10-min values. Conversely, the  $QP_{max}$  values fall below the results of consecutive maximum aggregation (D and L), where the relative deviation reaches 29 % for the 100<sup>th</sup> percentile.

The results show a similar tendency for both disturbance frequencies. The RMS aggregation at the last aggregation stage (A, C, E, G, I, K) results in the lowest deviation range ( $\pm 5\%$ ) for 99<sup>th</sup> percentile values.

Similar conclusions have been obtained from the analysis of daily measurements.

#### 4.3. EV chargers

The results are presented in Table 2. The  $QP_{max}$  values observed at the frequencies with highest disturbance levels during the measurement period of one day are 0.075 V (10 kHz), 0.178 V (18 kHz), and 0.166 V (36 kHz), which is clearly below the corresponding compatibility levels for non-intentional emission (2.8 V, 2.1 V and 1.1 V respectively).

The size of deviation ranges for 95<sup>th</sup> and 99<sup>th</sup> percentiles of aggregated values is larger than in the previous case due to the relatively short operation time of EV chargers during the day. The  $QP_{max}$  value exceeds the 95<sup>th</sup> percentile of consecutive RMS aggregated values by at least 20 %. Conversely, the consecutive maximum aggregation still provides a conservative estimate of  $QP_{max}$  with a relative deviation of 23 % for the 100<sup>th</sup> percentile.

The results of the analysis differ between disturbance frequencies. While the 99<sup>th</sup> percentile has the lowest deviation for disturbances around 10 kHz, the 100<sup>th</sup> percentile is a better representative for disturbances around 18 and 36 kHz. This difference is linked to the disturbance source (i.e. slow and fast chargers) and disturbance duration. The maximum

aggregation at the last aggregation stage ( $F, H, J, L$ ) provides the closest estimate of the  $QP_{\max}$  values for both disturbance sources. In these cases, the relative deviation for 99<sup>th</sup> percentile values does not exceed  $\pm 10\%$ .

#### 4.4 Discussion

The results indicate clear differences between the CISPR method and extension of IEC 61000-4-7 method. The relative deviations show similar tendencies for both considered disturbance sources but have different values.

The  $QP_{\max}$  values consistently exceed 95<sup>th</sup> and 99<sup>th</sup> percentiles of consecutive aggregated RMS values and may overestimate the possible impact of disturbances on additional thermal stress of connected electronic equipment. The deviation range tends to increase for disturbance sources with short operation time, e.g. EV chargers. The  $QP_{\max}$  values fall below the 100<sup>th</sup> percentile of consecutive aggregated maximum values and may underestimate the possible malfunction rate of connected electronic equipment.

High percentiles of aggregated values provide an estimate of the  $QP_{\max}$  values with moderate relative deviation. Selection of probability value and aggregation method for the closest estimate depends on characteristics of disturbance source, whereas the conservative estimate is always 100<sup>th</sup> percentiles of consecutive aggregated maximum values.

Although the IEC 61000-4-7 method is not able and not supposed to represent the  $QP_{\max}$  value, it can be used in a wide range of measurement cases, where accurate  $QP_{\max}$  measurement is not required. It properly reflects the common disturbance phenomena, it can be used in troubleshooting measurements to detect disturbers and it can even be applied for compliance assessment with compatibility levels, if the disturbance levels are clearly below the compatibility levels. Considering the computational requirements for implementing the CISPR method and proposed extension of IEC 61000-4-7 method, the latter would even be suitable to be included in IEC 61000-4-30 definition of class S instrument, providing more flexibility for the instrument manufacturers to offer instruments covering the 2-150 kHz range in different price segments.

## 5. Conclusion

This study evaluates the suitability of two methods for the measurement of disturbances in the frequency range 2-150 kHz for measuring grid disturbance levels. They are derived from the specifications in the standards CISPR 16-1-1 and IEC 61000-4-7. Based on long-term measurement of network disturbances at the point of connection of PV inverters and EV chargers, the ability of measurement methods to reflect relevant interference mechanisms and their suitability for assessment against compatibility levels are evaluated.

The measurement results of CISPR method are suitable for assessment against compatibility levels but may misinterpret relevant interference mechanisms. The analysis has shown that it may overestimate possible additional thermal stress of electronic equipment and underestimates the severity of disturbances concerning possible malfunction rate. The measurement results of IEC 61000-4-7 method are reflective

of interference mechanisms but have a limited application for the assessment of disturbance levels against compatibility levels. The analysis has shown that 99<sup>th</sup> and 100<sup>th</sup> percentiles of maximum aggregated values provide reliable conservative estimate of the quasi-peak values. This feature can be used as a practical and cost-effective alternative to CISPR method, i.e. for IEC 61000-4-30 class S measurement instruments.

The presented results shall contribute to the ongoing discussion towards a normative measurement method for the frequency range 2-150 kHz for the next edition of IEC 61000-4-30. The next steps include the analysis to further long-term measurements particularly including narrowband PLC signals. Detailed research on characteristics of network disturbance in the time domain and advanced procedures for more accurate estimation of the quasi-peak values are further ongoing activities.

## 6. Acknowledgements

The project 18NRM05 SupraEMI has received funding from the EMPIR programme co-financed by the Participating States and from the European Union's Horizon 2020 research and innovation programme. This work was funded in part by the Spanish Government under Grant RTI2018-099162-B-I00 (MCIU/AEI/FEDER-UE).

Authors like to thank utilities NetzeBW GmbH and SachsenEnergie AG for their support with the measurements.

## 7. References

- [1] CISPR Standard 16-1-1: 'Radio disturbance and immunity measuring apparatus', 2015.
- [2] IEC Standard 61000-2-2: 'Compatibility levels for low-frequency conducted disturbances and signalling in public low-voltage power supply systems', 2018.
- [3] Ritzmann, D., Lodetti, S., de la Vega, D., et al.: 'Comparison of measurement methods for 2-150-kHz conducted emission in power networks', IEEE Trans. on I&M, 2021, 70, pp. 1–10.
- [4] IEC Standard 61000-4-7: 'General guide on harmonics and interharmonics measurements and instrumentation, for power supply systems and equipment connected thereto', 2008.
- [5] IEC Standard 61000-4-30: 'Power quality measurement methods', 2015.
- [6] Klatt, M., Meyer, J., Schegner, P., et al.: 'Filter for the Measurement of Supraharmonic in Public Low Voltage Networks', Proc. Int. Symp. Electromagn. Compat. (EMC), Dresden, Germany, Aug 2015, pp. 108–115.
- [7] IEC, 'CISPR technical reports, CISPR/TR 16-3', 2010.
- [8] Krug, F., Müller, D., Russer, P.: 'Signal processing strategies with the TDEMI measurement system', IEEE Trans. on I&M, 2004, 53, (5), pp 1402-1408.
- [9] Khokhlov, V., Meyer, J., Schegner, P., et al.: 'Immunity assessment of household appliances in the frequency range 2-150 kHz', Proc. Int. Conf. CIRED, Madrid, Spain, Jun 2019, pp. 1–5.